Available online at www.sciencedirect.com
ScienceDirect
Trans. Nonferrous Met. Soc. China 26(2016) 2347−2354
Transactions of Nonferrous Metals Society of China
www.tnmsc.cn

Microstructure and properties of alloying coating on AZ31B magnesium alloy

Fen-jun LIU[1], Qing-sen MENG[2], Zeng-sheng LI[1]

1. College of Energy Engineering, Yulin University, Yulin 719000, China;
2. College of Materials Science and Engineering, Taiyuan University of Technology, Taiyuan 030024, China

Received 28 September 2015; accepted 14 June 2016

Abstract: Vacuum thermal diffusion technique was applied to preparing alloying coating on AZ31B magnesium alloy. The microstructure and phase composition of the coatings prepared at different holding time were investigated in detail using optical microscopy (OM), scanning electron microscopy (SEM), energy dispersive spectrometer (EDS) and X-ray diffraction (XRD), and so on. The microhardness tester and electrochemical workstation (PS−168a) were used to measure the microhardness and corrosion resistance of the alloying coating. The results showed that the alloying coatings gradually generated with the extension of holding time under constant temperature. And the obvious bonding interface between the coating and substrate was observed, and the bonding interface was changed from smooth to zigzag. EDS and XRD analyses showed that the microstructure of alloying coating mainly consisted of eutectic α-Mg phase and continuous network β-$Al_{12}Mg_{17}$ phase. The average microhardness of the coatings increased by 113% in comparison to the substrate, and the self-corrosion potential increased from −1.389 to −1.268 V at the same time.

Key words: AZ31B magnesium alloy; vacuum diffusion; surface alloying; microhardness; corrosion resistance

1 Introduction

Magnesium, which is one of the lightest engineering metals, exhibits special properties when it is alloyed with aluminium, zinc, manganese, rare earths, etc [1,2]. Magnesium alloys, therefore, are widely applied in transportation and aerospace industries. Especially, for the automobile industry, the average use of magnesium alloys per car has significantly increased [1,3]. However, the relatively poor corrosion resistance of magnesium alloys has been a serious impediment against its wider application. According to the previous research, it is considered to be two main reasons for the poor corrosion resistance of magnesium alloys [4]. One is the internal galvanic corrosion caused by second phases or impurities. The other is that the stability of quasi-passive hydroxide film on the surface of magnesium is much lower than that on aluminium and stainless steels, which makes the pitting resistance for magnesium and its alloys poor [5]. Therefore, the improvement of the corrosion resistance has become a key issue to expand the applications of magnesium alloys.

In order to improve the corrosion resistance, surface treatments, such as surface hardening process, anodizing, plating, spraying and physical vapor deposition (PVD), are usually used to form the passivation layer films on the surface of magnesium alloys. However, thin films prepared using these methods are normally insufficient in machine parts used under harsh conditions. For example, vapor coatings by PVD are too thin to endure under large stress. The adherence strength of the coatings prepared by plating method has a high probability to peel off during the service. Laser surface melting is employed to prepare a modified layer with the thickness of 283 μm for improving the surface properties of magnesium alloy [6]. However, the high expense of the instrument as well as the harmful substances generated during the fabrication process limited the development of this technology. Diffusion coating process, which is one of the most promising surface treatment methods, has been developed to modify the surface of magnesium alloys due to its high adherence strength and low equipment costs [7−13].

The diffusion coating process has been widely used in various alloy systems. Pure magnesium [7,13] and

Foundation item: Project (2015GY167) supported by the Science and Technology Department of Shaanxi Province, China; Project (2014cxy-05-1) supported by the Science and Technology Bureau of Yulin, China
Corresponding author: Fen-jun LIU; Tel: +86-18091231515; E-mail: lfjxcmg@126.com
DOI: 10.1016/S1003-6326(16)64353-4

AZ91D magnesium alloy [14,15] were embedded into aluminium powder by diffusion treatment in vacuum. Aluminized coating with free defects was prepared on magnesium alloy. And the coated specimen was much more corrosion resistant and harder than the uncoated one. The same researches were performed on the surface of pure magnesium [12], ZM5 [8] and AZ91E [9] magnesium alloy, treated in Al−Zn mixed powder to improve corrosion and wear resistance. It is shown that the Mg−Al−Zn intermetallic compound layer was found to be an effective corrosion barrier to decrease the corrosion rate [8]. Thus, vacuum thermal diffusion employed to prepare modified coating on magnesium alloy is effective and feasible.

In the present work, the aluminium powder was coated on the surface of AZ31B magnesium alloy by using liquid phase vacuum thermal diffusion technique. The microstructure and phase composition of the interface between the surface-alloyed coating and substrate were investigated, respectively. In addition, the microhardness of cross-section and corrosion resistance of alloyed coating were also examined. The corrosion resistance mechanism of alloyed coating was discussed in detail.

2 Experimental

The substrate selected for this work is AZ31B extruded plate with the thickness of 10 mm. Aluminium powder with the purity of 99.5% and particle size of 75−80 μm was used to prepare coating. Before vacuum thermal diffusion, the specimens (20 mm × 20 mm × 10 mm) were ground with 800, 1500 and 2000 grit SiC waterproof abrasive papers and cleaned by acetone, alcohol and deionized water in turn. Meanwhile, the Al powder was mixed with ethylene glycol to starchiness. Then, the AZ31B specimen with Al powder starchiness coated on the polished surface was embedded into crucible and put into vacuum resistance furnace, as shown in Fig. 1. The vacuum and heating temperature were fixed at $(2.2-2.4)\times10^{-2}$ Pa and 480 °C, respectively. The holding time was set to be 45, 50, 60, 90, 180 and 360 min, respectively.

The microstructure of the coating was investigated immediately by using JVC optical metallurgical microscope. The bonding interface and element distribution of the specimens were analyzed by using the LEO−438VP scanning electron microscope equipped with energy-dispersive spectrometer. Meanwhile, Y−2000 type X-ray diffractometer was also employed to investigate the phase composition of the coatings at a potential of 40 kV and current of 60 mA. The microhardness was evaluated by using a HXD−1000TM microhardness tester with the load and dwell time of 0.98 N and 15 s, respectively. The corrosion resistances of the specimens were assessed from potentiodynamic polarization test which were performed using PS−168a electrochemical corrosion test system in 5% NaCl solution at room temperature. The samples with an exposed area of 1 cm^2 were immersed into the solution. Each electrochemical measurement was implemented using a typical three-electrode cell system with the sample as the working electrode, the platinum plate as the auxiliary electrode and the Ag/AgCl (saturated with KCl) electrode as the reference electrode. All the electrochemical tests were carried out at a scanning rate of 1 mV/s.

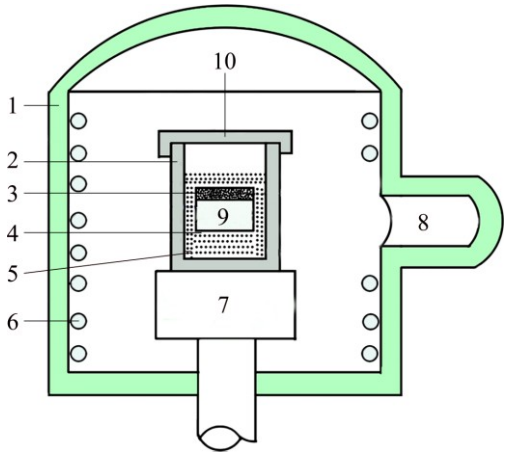


Fig. 1 Schematic diagram of surface alloying process: 1—Cavity; 2—Crucible; 3—Aluminium coating; 4—Thermo-couple; 5 — Aluminium powder; 6 — Molybdenum wire; 7—Lifting platform; 8—Vacuum system; 9—AZ31B substrate; 10—Sealing cover

3 Results and discussion

3.1 Microstructure of alloying coating

Figure 2 illustrates the microstructure of the alloying coating and bonding interface between the coating and substrate after thermal diffusion treated at

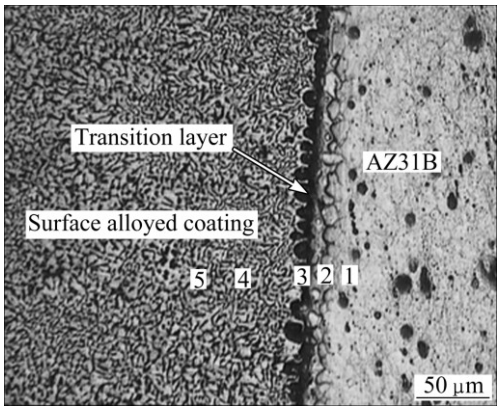


Fig. 2 Microstructure of surface alloying coating at holding time of 180 min

480 °C for 180 min. As can be seen from the figure, the region consists of AZ31B substrate, transition layer and alloying coatings. The transition layer which plays a very important role in the bonding strength between coating and substrate exhibits zigzag columnar or cell structure. For the alloying coating, it reveals a continuous chrysanthemum structure located at the outmost of the magnesium alloy surface.

As can be seen from Figs. 3(a) and (b), the alloying coating is not generated with the holding time increasing from 45 to 50 min. When the holding time reaches 60 min, the coating has already formed on the surface of magnesium alloy. The thickness and morphology of the coating change obviously with the increment of holding time. After holding for 60 min, the transition layer with the thickness of 10−15 μm exhibits a micro cellular protrusions status in Fig. 3(c). When the holding time reaches 90 min, the growth of cellular dendrite along the interface plane causes the formation of a flat belt with the thickness of 16−20 μm. After holding for 180 min, the thickness of the transition layer reaches 25−30 μm, exhibiting a cellular or columnar shape. The thickness of the transition layer increases sharply to 500 μm when holding for 360 min. Besides, the microstructure of transition layer close to the substrate is the same as that of the substrate. Based on the EDS analysis for the coating and the interface, it is found that the transition layer is composed of α-Mg phase. It can be speculated that the inter-diffusion process happens between Mg and Al atoms with the driving force of concentration gradient. TAN et al [16] have already confirmed that the inter-diffusion and crystalline between Mg and Al atoms will lead to the formation of diffusion dissolution layer on the surface of AZ31 magnesium alloy. As Al atoms

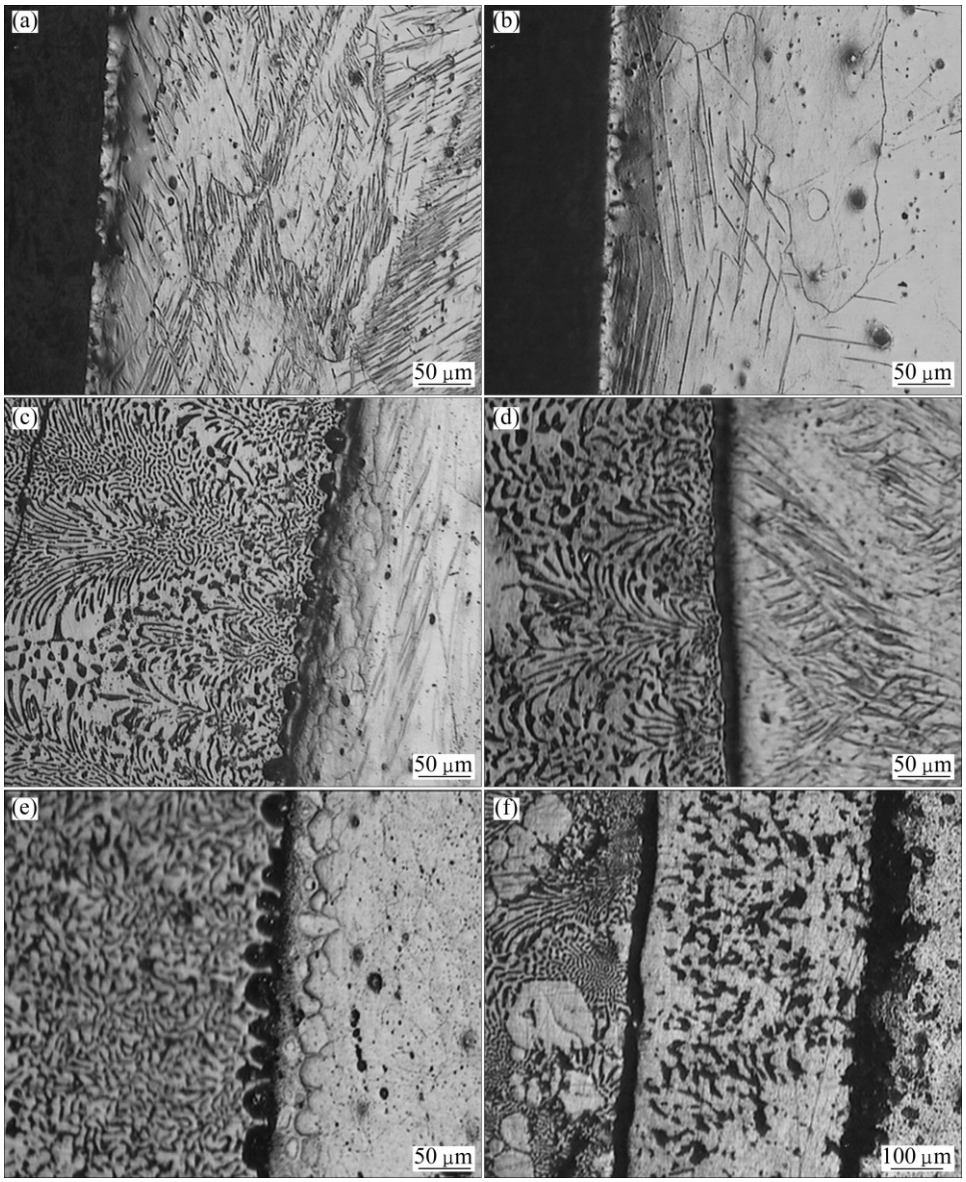


Fig. 3 Microstructures of transition layer at different holding time: (a) 45 min; (b) 50 min; (c) 60 min; (d) 90 min; (e) 180 min; (f) 360 min

diffuse into AZ31B substrate continuously, the transition layer emerges at the initial contact interface. The EDS results of positions 2 and 3 (Fig. 2) indicate that the mole fraction of Al element in the corresponding area is 7.4% from Fig. 4. According to the Mg−Al equilibrium phase diagram [17], it is known that the transition layer is determined to be α-Mg phase.

As the transition layer connects the substrate and coating, the bonding interface structure is quite important for the bonding strength. The SEM image in Fig. 5(a) suggests a zigzag status between transition layer and the substrate in the interface region for the sample with the holding time of 360 min. This is beneficial to the bonding strength between transition layer and the substrate. However, the interface between transition layer and the coating exhibits a much smoother state. The reason for the two types of interfaces is considered to be different growth speeds of the formed new phase during the preparation of the coating. Under full thermal insulation conditions, the supersaturated solid solution will form at the interface. As the temperature of preparing the coating exceeds the Mg−Al eutectic temperature of 437 °C, the liquid phase appears at the interface, leading to the formation of zigzag status. The growth speed of the cellular or columnar structure towards the coating is much lower at the interface

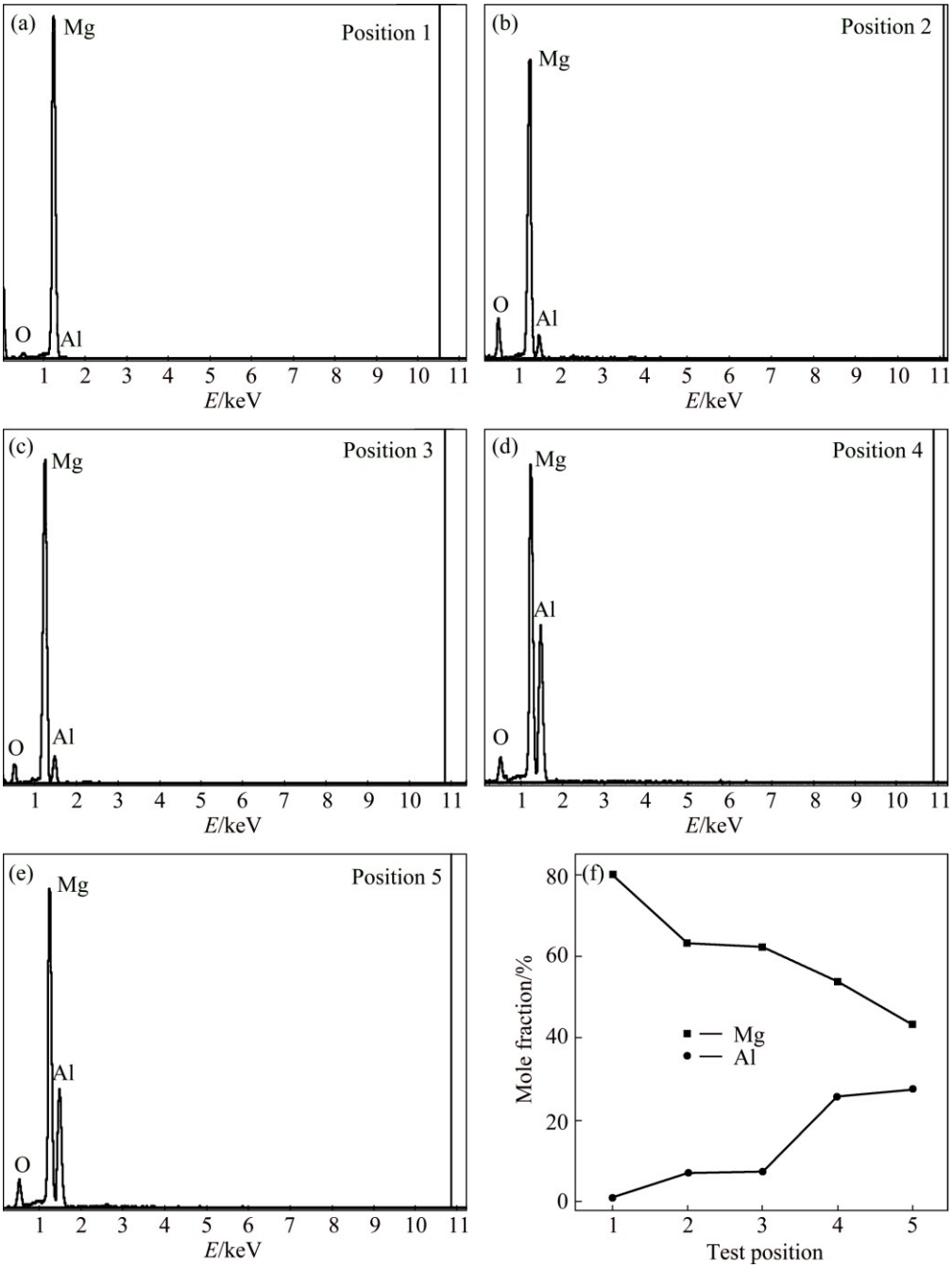


Fig. 4 Mole fractions of Mg and Al near interface surface alloying coating and matrix by EDS

between the transition layer and the alloying coating than that along the perpendicular direction. This will finally lead to the formation of smooth interface, as indicated in Fig. 5(b).

The microstructures of the alloying coating, which present network structure in the shape of chrysanthemum, are shown in Fig. 6. In addition, the contents (mole fraction) of Al at Points 4 and 5 in Fig. 2 are gotten to be about 29.8% and 31.6% by EDS, as shown in Fig. 4, respectively. According to the Mg−Al equilibrium phase diagram, the maximum solubility of Al in Mg−Al alloy is 12.4%. The Al contents for these two points are significantly higher than 12.4%. The over-saturated solid solution region is located in the coexistent area of solid and liquid phases. It can lead to the melting of some regions on the surface of magnesium alloy. Under the effect of liquid phase surface tension, the Mg atoms dissolve into the melted zone, while Al atoms also spread into the magnesium substrate at the same time. With the exceeding of holding time, the liquid phase region increases significantly. When the temperature decreases to 437 °C, the eutectic reaction ($L \rightarrow Al_{12}Mg_{17} + \alpha$-Mg) happens, leading to the formation of eutectic structure in the shape of chrysanthemum. This is fully consistent with the XRD results, as shown in Fig. 7. α-Mg and $Al_{12}Mg_{17}$ are phases existing in alloying coating and as-received AZ31B magnesium alloy. The amount of $Al_{12}Mg_{17}$ existing in the alloying coating is larger than that of α-Mg. The Al contents for these specimens are all higher than 12.4%. In this situation, it is beneficial for Al combining with Mg to form $Al_{12}Mg_{17}$. The diffraction peaks from α-Mg and $Al_{12}Mg_{17}$ phases were used to estimate the volume fraction x_1 of $Al_{12}Mg_{17}$ by following equation [18]:

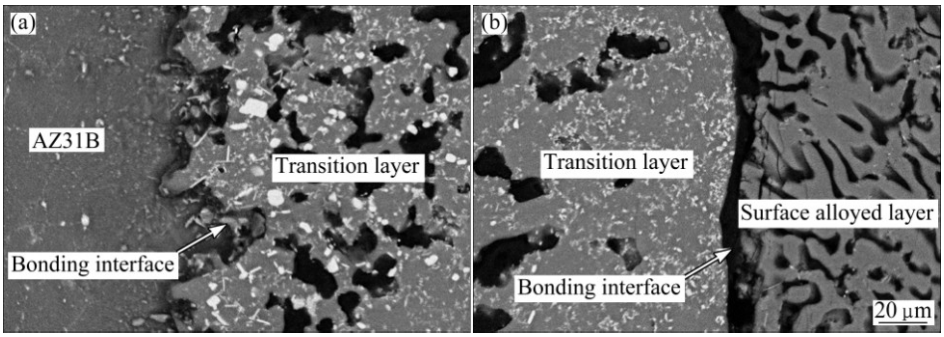


Fig. 5 Bonding interface microstructures: (a) Between transition layer and matrix alloy; (b) Between surface alloyed layer and transition layer

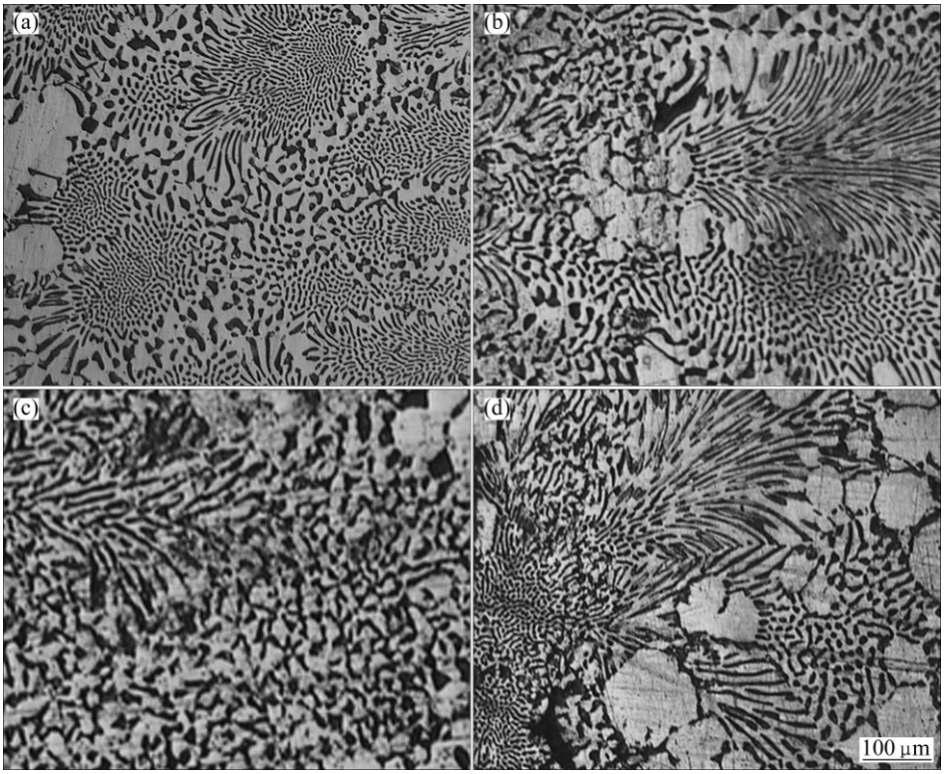


Fig. 6 Microstructures of surface alloying coating at different holding time: (a) 60 min; (b) 90 min; (c) 180 min; (d) 360 min

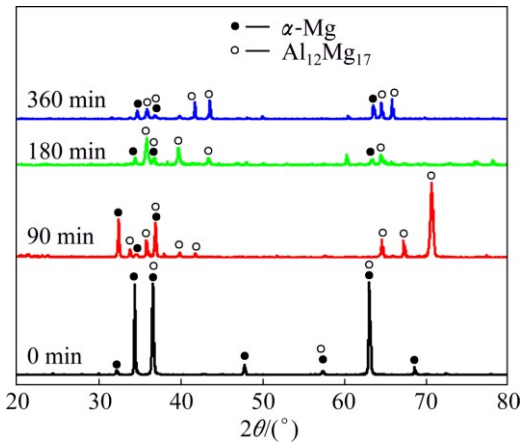


Fig. 7 XRD patterns of surface alloying coating at different holding time

$$x_i = \frac{1}{(K_i/I_i)\sum_{i}^{n}(I_i/K_i)} \quad (1)$$

where K_i and I_i are the percentages of reference intensity and diffracted intensity, respectively. The volume fraction of $Al_{12}Mg_{17}$ for the specimens at different holding time was calculated. With increasing the Al content, more $Al_{12}Mg_{17}$ appears. This is because Al−Mg liquid with higher Al content is closer to $Al_{12}Mg_{17}$ phase region in Al−Mg equilibrium phase diagram and favors to form more $Al_{12}Mg_{17}$.

3.2 Microhardness

Figure 8 presents the microhardness profiles of the vacuum thermal diffusion AZ31B magnesium alloys under different holding time, as a function of distance from the surface measured on the cross-sectional plane in the surface alloying coating. It is obvious that the microhardness of the alloying coating has significantly increased by 1.6−2.5 times (HV 85−130), as compared to that of the as-received AZ31B magnesium alloy (HV 53). The maximum microhardness of the alloying coating is close to that of the surface and decreases quickly between the interface of alloying coating and substrate. This improvement in microhardness may be attributed to the formation of intermetallic compound (β-$Al_{12}Mg_{17}$). In addition, the maximum microhardness in the surface alloying coating seems to vary with the holding time. The maximum microhardness is achieved following vacuum thermal diffusion with long holding time. As holding time extends, the number of β-$Al_{12}Mg_{17}$ phase in the alloying coating increases. The presence of massive β-$Al_{12}Mg_{17}$ compounds inside the coating can significantly improve the microhardness [8,14]. Hence, it may be concluded that the significant enhancement in microhardness improved by the formation of massive β-$Al_{12}Mg_{17}$ phase may be effective in imparting a better resistance to corrosion in AZ31B magnesium alloy.

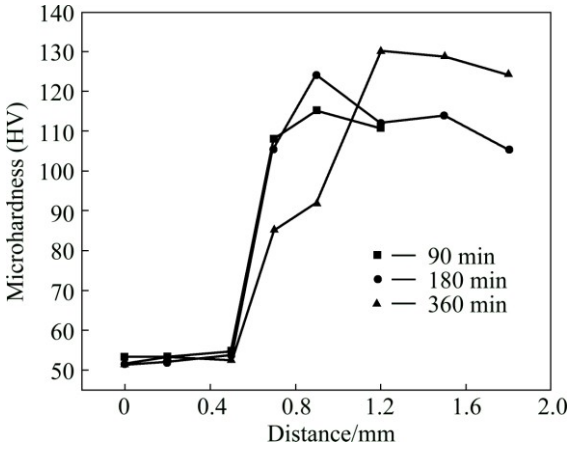


Fig. 8 Microhardness distribution of surface alloyed coating at different holding time

3.3 Corrosion resistance

The corrosion resistance of magnesium alloys depends on the properties of the film developed by vacuum thermal diffusion to which they are exposed. In general, it is shown that the existence of aluminium in signal-phase Mg−Al alloys has a positive influence on the corrosion behaviour in chloride media. And this behaviour has been clearly revealed for AZ31B magnesium alloy, which performed higher corrosion resistance than commercially pure Mg [19]. In the present work, the coatings prepared on the surface of AZ31B magnesium alloy by vacuum thermal diffusion technique under different conditions were soaked in the 5% NaCl solution at room temperature to ascertain the corrosion resistance. Polarization curves and corrosion potentials of the coatings are shown in Fig. 9 and Table 1, respectively. From Table 1, it is noticed that the corrosion potential of the diffusion-treated specimen is 0.121 V higher than that of the bare AZ31B specimen.

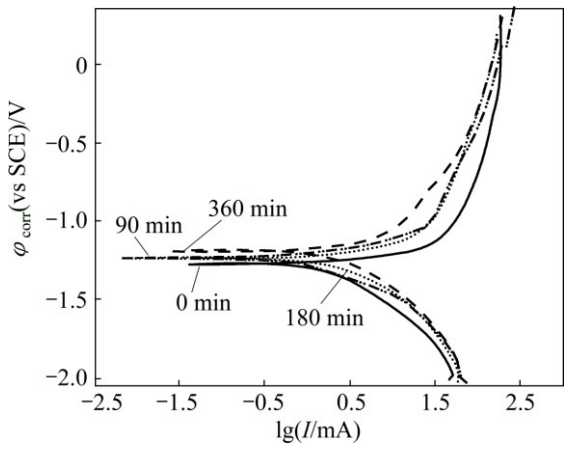


Fig. 9 Potentiodynamic polarization curves of surface alloyed coating at different holding time and matrix AZ31B

Table 1 Corrosion potential (φ_{corr}) of surface alloyed coating at different holding times in 5% NaCl solution

Holding time/min	φ_{corr} (vs SCE)/V
0	−1.389
90	−1.314
180	−1.290
360	−1.268

And it is also found that the self-corrosion potential increases with the increment of the holding time. In addition, all the corrosion potentials are greater than those of the magnesium alloy substrate. This indicates that the β-$Al_{12}Mg_{17}$ alloying coating formed with continuous network distribution, by which the corrosion to the substrate will be blocked. With the increment of the holding time, the quantity of β-$Al_{12}Mg_{17}$ phase increases significantly, leading to the increase of self-corrosion potential of the alloying coating surface.

When the as-received magnesium alloy is exposed to the atmosphere or aqueous solutions, magnesium hydroxide and hydrogen gas are produced by an electrochemical reaction with water. The corrosion attack in aqueous environment often involves micro- galvanic coupling between anodic and cathodic areas.

$$Mg \rightarrow Mg^{2+}+2e \text{ (Anodic reaction)} \quad (2)$$

$$2H_2O+2e \rightarrow H_2+2OH^- \text{ (Cathodic reaction)} \quad (3)$$

Thus, the overall reaction may be expressed as

$$Mg^{2+}+2OH^- \rightarrow Mg(OH)_2 \text{ (Corrosion product)} \quad (4)$$

Magnesium hydroxide formed on the bare surface, which is stable for the basic range of pH values [20]. Nevertheless, in presence of chloride anions, this surface film breaks down and magnesium appears unprotected. And a soluble magnesium salt is generated at the magnesium/solution interface by the following reaction:

$$Mg^{2+}+2Cl^- \rightarrow MgCl_2 \text{ (Corrosion product)} \quad (5)$$

This soluble magnesium salt destroys the magnesium hydroxide protective film, and the exposed magnesium alloy reacts with the electrolyte (self-dissolution) at sites where the protective film is breached. This local corrosion brings about formation of pits on the surface. Once the pit formation initiates, it propagates at a very rapid rate. SONG et al [21] found that the β-phase ($Al_{12}Mg_{17}$) had higher cathodic reaction activity than the α-phase (α-Mg), but its anodic dissolution rate was much lower (below its pitting potential) than that of α-phase. At their corrosion potentials, the corrosion current density of β-phase was much lower than that of α-phase. This means that β-phase was very stable in NaCl solution and was inert to corrosion. Previous investigations reported that the distribution of the β-phase ($Al_{12}Mg_{17}$) determined the corrosion resistance of the Mg−Al alloys [21−25]. According to the research results, for a low volume fraction, the β-phase plays a cathode role and accelerates the corrosion rate of the α-Mg; however, a large volume fraction serves as an anodic barrier and the general corrosion rate decreases. Moreover, it has also been found that the ratio of the β-phase to the surrounding Al-rich α-Mg or eutectic α-Mg plays an important role in the formation of the galvanic cells. Besides the microstructure, the composition of the corrosion layer may improve the corrosion resistance. For example, NORDLIEN et al [25] indicated that alumina components form a continuous skeletal structure in the oxide layer of the magnesium alloy, and its passivating properties are much better than those of $Mg(OH)_2$ and MgO layers. In the present work, the amount of $Al_{12}Mg_{17}$ in the alloying coating prepared at different holding time is larger than that of the as-received AZ31B magnesium alloy. The relatively large volume fraction β-$Al_{12}Mg_{17}$ phase network acts as an effective barrier against process of corrosion attack.

4 Conclusions

1) The surface alloying coating prepared on AZ31B magnesium alloy was confirmed to be the mixture of eutectic reaction structure α-Mg and β-$Al_{12}Mg_{17}$. The interface between the coating and substrate exhibits zigzag status.

2) The width of the coating increased with the increase of holding time. In addition, the microstructure of the transition layer located between coating and the substrate changed significantly with the variation of holding time.

3) The microhardness of the alloying coating is about 2.5 times than that of the substrate. Through the electrochemical corrosion test, it is found that the self-corrosion potential increased from −1.389 to −1.268 V. This can be attributed to the blocking effect of network shaped β-$Al_{12}Mg_{17}$ compounds distributed inside the coating.

References

[1] BLAWERT C, HORT N, KAINER K V. Automotive applications of magnesium and its alloys [J]. Transactions of the Indian Institute of Metals, 2004, 57: 397−408.

[2] ELIEZER D, AGHION E, FROES F H. Magnesium science, technology and applications [J]. Advanced Performance Materials, 1998, 5: 201−212.

[3] FRIEDRICH H, SCHUMANN S. Research for a “new age of magnesium” in the automotive industry [J]. Journal of Materials Processing Technology, 2001, 117: 276−281.

[4] MAKAR G L, KRUGER J. Corrosion studies of rapidly solidified magnesium alloys [J]. Journal of the Electrochemical Society, 1993, 137: 414−421.

[5] SONG G L, ATRENS A. Corrosion mechanisms of magnesium alloys [J]. Advanced Engineering Materials, 1999, 1: 11−33.
[6] CUI Z Q, SHI H X, WANG W X, XU B S. Laser surface melting AZ31B magnesium alloy with liquid nitrogen-assisted cooling [J]. Transactions of Nonferrous Metals Society of China, 2015, 25: 1446−1453.
[7] LIU F C, LI X R, LIANG W, ZHAO X G, ZHANG Y. Effect of temperature on microstructures and properties of aluminized coating on pure magnesium [J]. Journal of Alloys and Compounds, 2009, 478: 579−585.
[8] MA Y P, LI X L, YANG L, HE X P. Effect of surface diffusion alloying on erosion wear property of ZM5 magnesium alloy [J]. Transactions of Nonferrous Metals Society of China, 2013, 23: 323−328.
[9] HIRMKE J, ZHANG M X, STJOHN D H. Surface alloying of AZ91E alloy by Al−Zn packed powder diffusion coating [J]. Surface and Coatings Technology, 2011, 206: 425−433.
[10] HIRMKE J, ZHANG M X, STJOHN D H. Influence of chemical composition of Mg alloys on surface alloying by diffusion coating [J]. Metallurgical and Materials Transactions A, 2012, 43: 1621−1628.
[11] TACIKOWSKI M, MORGIEL J, BANASZEK M, CYMERMAN K, WIERZCHON T. Structure and properties of diffusive titanium nitride layers produced by hybrid method on AZ91D magnesium alloy [J]. Transactions of Nonferrous Metals Society of China, 2014, 24: 2767−2775.
[12] MOLA R. Fabrication and microstructural characterization of Al/Zn-enriched layers on pure magnesium [J]. Materials Characterization, 2013, 78: 121−128.
[13] MOLA R, JAGIELSKA-WIADEREK K. Formation of Al-enriched surface layers through reaction at the Mg-substrate/Al-powder interface [J]. Surface and Interface Analysis, 2014, 56: 577−580.
[14] SHIGEMATSU I, NAKAMURA M, SAITOU N, SHIMOJIMA K. Surface treatment of AZ91D magnesium alloy by aluminum diffusion coating [J]. Journal of Materials Science Letters, 2000, 19: 473−475.
[15] ZHU L Q, SONG G L. Improved corrosion resistance of AZ91D magnesium alloy by an aluminium-alloyed coating [J]. Surface and Coatings Technology, 2006, 200: 2834−2840.
[16] TAN C W, GUO G W, WANG X Y, WANG F C, CAI H N. Processes and properties of liquid aluminized coating on AZ31 magnesium alloy [J]. Transactions of Nonferrous Metals Society of China, 2007, 17: 1053−1057.
[17] MURRAY J L. Binary alloy phase diagrams [M]. 2nd ed. Ohio: ASM International, 1990.
[18] LIU Y H, GUO Z X, WANG H Y, HU J D, LI Y X. Laser (a pulsed Nd: YAG) cladding of AZ91D magnesium alloy with Al and Al_2O_3 powders [J]. Applied Surface Science, 2006, 253: 1722−1728.
[19] PARDO A, MERINO M C, COY A E, ARRABAL R, VOEJO F, MATYKINA E. Corrosion behaviour of magnesium/aluminium alloys in 3.5 wt.% NaCl [J]. Corrosion Science, 2008, 50: 823−834.
[20] SHAW B A. Corrosion resistance of magnesium alloys [M]. Ohio: ASM International, 2003.
[21] SONG G L, ATRENS A, WU X L, ZHANG B. Corrosion behaviour of AZ21, AZ501 and AZ91 in sodium chloride [J]. Corrosion Science, 1998, 40: 1769−1791.
[22] DUTTA MAJUMDAR J, GALUN R, MORDIKE B L, MANNA I. Effect of laser surface melting on corrosion and wear resistance of a commercial magnesium alloy [J]. Materials Science and Engineering A, 2003, 361: 119−129.
[23] ALVES H, KOSTER U, AGHION E, ELIEZER D. Environmental behavior of magnesium and magnesium alloys [J]. Material Technology, 2001, 16: 110−126.
[24] ZHANG T, LI Y, WANG F H. Roles of β phase in the corrosion process of AZ91D magnesium alloy [J]. Corrosion Science, 2006, 48: 1249−1264.
[25] NORDLIEN J H, ONO S, MASUKO N, NISANCIOGLU K. A TEM investigation of naturally formed oxide films on pure magnesium [J]. Corrosion Science, 1997, 39: 1397−1414.

AZ31B 镁合金表面合金化涂层的显微组织和耐腐蚀性能

刘奋军[1]，孟庆森[2]，李增生[1]

1. 榆林学院 能源工程学院，榆林 719000；
2. 太原理工大学 材料科学与工程学院，太原 030024

摘　要：通过真空热扩渗技术在 AZ31B 镁合金表面制备一层合金化涂层。采用 OM、SEM、EDS 及 XRD 等方法分析合金化涂层的显微组织、成分和相组成，并利用显微硬度计和 PS−168a 型电化学腐蚀测试系统分别对合金化涂层的显微硬度和耐腐蚀性能进行测试分析。研究结果表明：恒温条件下，随着保温时间的延长，在 AZ31B 镁合金表面可以形成合金化涂层。随着保温时间的延长，涂层与基体之间结合界面形貌由平直结合转变成“锯齿”状咬合；且合金化涂层与基体之间存在明显的过渡层，过渡层逐渐变宽。EDS 及 XRD 分析结果表明，合金化涂层为 Mg−Al 共晶组织 α-Mg 和 β-$Al_{12}Mg_{17}$，合金化涂层的平均显微硬度比基体的平均显微硬度提高了 113%；自腐蚀电位也由基体的−1.389 V 提高到−1.268 V。

关键词：AZ31B 镁合金；真空热扩渗；表面合金化；显微硬度；耐蚀性

(Edited by Wei-ping CHEN)